BMC Plant Biology

RESEARCH

Open Access

Dissolved inorganic carbon input significantly lowers carbon dioxide flux but not methane flux in shallow macrophyte-dominated systems with positive effects on carbon stocks

Fei Diao[1,2], Ailifeire Anwaier[1,2], Wenjuan Qiu[1,2], Tian Qian[1,2], Baohua Guan[1], Yaling Su[1*] and Kuanyi Li[1*]

Abstract

Background With the increase in the inorganic carbon input from watersheds, elevated dissolved inorganic carbon (DIC) concentrations will significantly impact the carbon cycle in freshwater ecosystems. Moreover, the limited diffusion rate of CO_2 in water, coupled with the lack of functional stomata, greatly restricts the ability of submerged macrophytes to absorb CO_2 from their aquatic environment. The importance of bicarbonate (HCO_3^-) for submerged macrophytes becomes more pronounced. Current research focuses on the effects of DIC (notably HCO_3^-) on the phenotypic plasticity of submerged macrophytes, while its impact on their carbon stock capabilities has rarely been reported.

Results In this study, *Myriophyllum spicatum* served as the model macrophyte within a mesocosm experimental system to assess the impact of HCO_3^- enrichment (0.5 to 2.5 mmol L^{-1}) on carbon stocks and emissions across a one-year period. Our findings indicated that the addition of HCO_3^- had a non-significant inhibitory effect on the diffusive fluxes of methane (CH_4) emissions. Concurrently, it significantly reduced CO_2 fluxes within the systems. The annual average CO_2 fluxes across the four HCO_3^- addition levels were -3.48 ± 7.60, -6.78 ± 5.87, -7.15 ± 8.68, and -14.04 ± 14.39 mol m^{-2} yr^{-1}, respectively, showing significant differences between low /medium- and high- HCO_3^- addition levels.

Conclusion The addition of HCO_3^- enhanced carbon stocks in water, macrophytes and the entire system, with minimal effects on carbon sedimentation stocks. Our study provides valuable insights into understanding the carbon sink capacity of aquatic ecosystems and elucidates the underlying mechanisms driving these processes on a system scale.

Keywords Carbon stock, Greenhouse gas flux, Dissolved inorganic carbon, Submerged macrophyte, Carbon sedimentation

*Correspondence:
Yaling Su
ylsu@niglas.ac.cn
Kuanyi Li
kyli@niglas.ac.cn
[1] Key Laboratory of Lake and Watershed Science for Water Security, Nanjing Institute of Geography and Limnology, Chinese Academy of Science, 299 Chuangzhan Road, Qilin Subdistrict, Jiangning District, Nanjing 211135, China
[2] University of Chinese Academy of Science, Beijing 100049, China

Introduction

Greenhouse gas (GHG) emissions from lakes constitute a crucial part of the global carbon budget. The annual emissions of CO_2 and CH_4 from global lakes are estimated at approximately 0.53 Pg C and 0.15 Pg C, respectively [44]. The carbon cycle within lakes significantly influences their GHG emissions. Carbon cycling encompasses various processes: the fixation of inorganic carbon by primary producers through photosynthesis, the conversion into various forms of organic carbon (OC), carbon emissions, and carbon sedimentation [63]. The effects of carbon decomposition are ultimately reflected in changes in organic or inorganic carbon concentrations in systems and CO_2 and CH_4 emissions [57, 59]. Lake carbon cycling can be greatly affected by external carbon inputs. It is estimated that at least 1.13 ± 0.33 billion tons of inorganic carbon, predominantly in the form of DIC, are annually lost to inland waters through soil erosion [20]. With the increase in inorganic carbon inputs, DIC has become increasingly significant for the photosynthetic carbon fixation of submerged macrophytes.

In the process of photosynthetic carbon fixation by submerged macrophytes, CO_2 is the most easily acquired form of inorganic carbon for it can enter the cells through passive transport [41]. Nonetheless, the diffusion rate of CO_2 in water is only one ten-thousandth of that in air. Submerged macrophytes lack functional stomata, which limited their ability to acquire CO_2 from water [37]. To address the stress of limited CO_2 availability in aquatic environments, submerged macrophytes have evolved a strategy to utilize bicarbonate (HCO_3^-) as an alternative carbon source for photosynthesis [39]. The comprehension of how DIC input influences the balance among carbon fixation, sedimentation, and emissions is crucial for predicting carbon stocks under global changes.

The impact of submerged macrophytes on CO_2 and CH_4 emissions is still under debate. DIC can promote the growth of macrophytes and enhance the conversion to higher levels of biological carbon bound in their biomass [34, 39]. These biological carbon compounds are often recalcitrant compounds (e.g., cellulose and lignin), thus they easily form refractory carbon pools and thereby increasing carbon stock capacity [26, 54]. However, the increase in submerged macrophyte biomass also implies a rise in CO_2 and CH_4 produced through their respiration and decomposition after decay [12]. Additionally, the increase in submerged macrophyte biomass may directly or indirectly promote CH_4 formation via aerobic methanogenesis or co-metabolic effects [1, 42]. Submerged macrophytes might directly contribute to CH_4 formation by generating strong oxidants that drive methyl radical production to form CH_4 [17]. Some perspectives suggested that submerged macrophytes had an insignificant impact on lake CO_2 and CH_4 emissions, regardless of short-term effects over three months [14, 16] or long-term effects over one year [2]. However, other perspectives argued that an increase in submerged macrophyte biomass can enhance CH_4 emissions while reducing CO_2 emissions [58]. The impact of submerged macrophytes on CO_2 and CH_4 emissions, as well as the mechanisms driving such effects, remains unexplored in the context of external DIC input. Thus, a detailed understanding of how HCO_3^- affects carbon cycling is important to predict how DIC will influence carbon stocks in lakes.

To date, few comprehensive studies have explored the effects of DIC, particularly HCO_3^-, on carbon stocks and emissions in submerged macrophyte-dominated systems. To address this research gap, we conducted a year-long 450 L mesocosm experiment to investigate the influence of HCO_3^- on carbon stocks as well as CO_2 and CH_4 fluxes. The experiment employed *Myriophyllum spicatum* (*M. spicatum*), a submerged, rooted freshwater plant species widely distributed across Europe, Asia, and North America, renowned for its efficient utilization of HCO_3^- [62]. The mesocosms were subjected to subtropical (China) conditions with three different HCO_3^- addition scenarios (0.5, 1.0, and 2.5 mmol L^{-1}). During the experiment, we measured biomass and carbon content of macrophytes, CO_2 and CH_4 fluxes, and the weight and carbon content of sedimental material. We also quantified the abundance of zooplankton, phytoplankton, and genes related to methanogenic and methanotrophic microorganisms. We hypothesized that increased macrophytes biomass due to HCO_3^- addition would enhance the system's carbon stocks through the conversion of biomass carbon, and that could uptake more HCO_3^- and thus reduce CO_2 flux. However, we postulated that this increase in biomass would have non-significant effects on CH_4 flux. We identified the key predictors of CH_4 and CO_2 fluxes following HCO_3^- addition. To determine the net carbon stock of the system throughout the experiment, we integrated sedimentation, plant carbon fixation, carbon concentration in the water body into a carbon stock model.

Methods

Experimental set-up

The outdoor mesocosm experiment was conducted at Dongshan substation of Taihu Lake Ecosystem Research Station (31°2′2″N, 120°25′17″E) in Jiangsu Province, China, from July 2023 to August 2024. The mesocosms comprised 16 opaque polyethylene barrels, each with a top diameter of 100 cm, a bottom diameter of 85 cm, and a depth of 83 cm. Prior to the experiment, *M. spicatum* was collected from Eastern Lake Taihu and pre-cultivated in a barrel for two months. Sediments collected

from Eastern Lake Taihu were spread on outdoor concrete surfaces to air dry under sunlight for 15 days, effectively minimizing the influence of benthic animals and aquatic plant seeds on the experiment. Larger debris such as dead branches, stones, and remnants of benthic fauna were manually selected and removed. The dried sediments were then placed in the barrels, and 450 L of lake water was pumped from the surface of Eastern Lake Taihu. The barrels were then left to stand for three days to allow the sediment to fully rehydrate. A mixer was used to homogenize the sediments, breaking down larger clumps into fine particles. The barrels were left undisturbed for an additional ten days to facilitate the settling of suspended sediment particles and to clarify the water. Throughout this period, floating debris and dead branches were removed from the water surface by a scoop net. Subsequently, *M. spicatum* of uniform height and biomass was selected from the pre-culture barrel and transplanted in a concentric circle pattern within the cleared barrels using the cutting method. Each barrel received 20 unbranched shoots of *M. spicatum*, with an average total biomass of 40.24 ± 0.36 g (fresh weight) and an average height of 26.56 ± 1.73 cm. Post-planting, the macrophytes were left undisturbed for one week to acclimate to their new environment. During the acclimation period, any macrophytes that failed to adapt were promptly replaced with fresh ones under the same conditions. Once the experimental system was successfully established, a beaker (7 cm in diameter, 9.9 cm in height, and 250 mL in volume) was embedded in the sediment of each barrel to collect sediments over the duration of the one-year study.

A one-way factorial experiment was designed with four levels of HCO_3^- addition (0 mmol L^{-1}, 0.5 mmol L^{-1}, 1 mmol L^{-1}, and 2.5 mmol L^{-1}, designated as "Control", "Low", "Medium", and "High", respectively). Each treatment had four replicates. HCO_3^- was introduced as $NaHCO_3$. For each treatment, a precise quantity of $NaHCO_3$ powder (Sinopharm, AR) was weighed, dissolved in water, and then added to each experimental barrel, ensuring thorough mixing. Following the addition of HCO_3^-, the pH values of each treatment were 7.04 ± 0.13, 7.45 ± 0.22, 7.63 ± 0.25, and 8.06 ± 0.34, respectively, which are consistent with the range typically observed for pH levels in natural waters [51]. Initially, HCO_3^- was added once in August 2023. The addition was halted as the plant growing season drew to a close. From March 2024 to July 2024, monthly HCO_3^- additions were resumed.

The experiment was conducted over a full year, encompassing the growth and decay periods of *M. spicatum*. Throughout the duration of the experiment, water transparency in each experimental barrel was consistently sufficient to allow visibility to the bottom (approximately 70 cm). The total nitrogen concentration in the water was sustained at 0.75 ± 0.47 mg L^{-1}, and the total phosphorus concentration was kept at 0.033 ± 0.025 mg L^{-1}. These conditions were adequate to fulfill the light and nutrient requirements necessary for the normal growth of *M. spicatum*. During the experiment, water levels in the experimental barrels were kept relatively consistent. Natural rainfall was utilized to replenish water levels, and when rainfall was scarce, tap water was promptly added to prevent significant deviations in water levels. Additionally, the cylinder walls were regularly cleaned to mitigate the impact of periphyton on the experimental results.

Water quality parameters

Water temperature (WT), pH, dissolved oxygen (DO), salinity (SAL) and specific conductance were measured by a portable multiparameter water quality meter (YSI ProQuatro, YSI Inc., USA). Raw water samples were analyzed for total nitrogen (TN), total phosphorus (TP), total organic carbon (TOC), total inorganic carbon (TIC) and alkalinity. To determine dissolved total nitrogen (DTN) and dissolved total phosphorus (DTP), water samples were filtered through GF/C filters (1.2 μm, Whatman, UK). The GF/C filters were subsequently used for chlorophyll-*a* (Chl-*a*) determination. For dissolved organic carbon (DOC) and dissolved inorganic carbon (DIC) analysis, water samples were filtered through GF/F filters (0.7 μm, Whatman, UK). TN, TP, DTN, DTP and Chl-*a* were analyzed with a UV spectrophotometer (UV2600, Shimadzu, Japan). Alkalinity was determined by acid–base titration [43]. TOC, TIC, DOC and DIC were analyzed by high-temperature oxidation method with a TOC analyzer (TOC-L CPH, Shimadzu, Japan). All the aforementioned water quality parameters were measured once a month.

Carbon sedimentation and content in sediments

Following the conclusion of the one-year experiment, the beakers embedded in the sediments were retrieved and transported to the laboratory. The beakers were left to stand for three days to facilitate the settling of suspended particles in the overlying water. The water was then carefully siphoned off, and the beakers were dried externally. The total wet weight of the sediment was recorded using an electronic balance. Subsequently, a sufficient portion of the sediment was placed in an oven at 105°C for 48 h to achieve a constant weight, after which the dry weight was measured. The dried sediment was ground using an agate mortar and passed through a 100-mesh sieve. Finally, the total carbon content of the sediments was determined using an organic elemental analyzer (Vario UNICUBE, Elementar, German).

CH_4 and CO_2 diffusive fluxes at the water–air interface

Given that the diffusive flux is at least three orders of magnitude higher than the ebullition flux (Table S1), this study chose to focus solely on the diffusive flux. Diffusive fluxes of CH_4 (FCH_4) and CO_2 (FCO_2) were measured once a month. The measurements of FCH_4 and FCO_2 at the water–air interface were performed using the static chamber method. A portable GHG analyzer (GW-2032, Wuhan Ganwei Technology Co., Ltd., China) was utilized to measure the real-time concentration of CH_4 and CO_2 accumulated in the floating chamber of each experimental barrel. The floating chamber design, as described by Xun et al. [61], consisted of a plexiglass cylindrical barrel, a lid with a fan gas mixing, an air inlet, an air outlet duct, and a floating ring.

The concentration of CH_4 and CO_2 accumulated in the floating chamber were employed to calculate the FCH_4 and FCO_2. The calculation was performed as follows:

$$F = \frac{(C_2 - C_1) \bullet h}{\Delta t \bullet V_m} \bullet \frac{T_1}{T_2} \bullet \frac{P_2}{P_1}$$

where F is the FCH_4 and FCO_2 (μmol m^{-2} s^{-1} or mol m^{-2} yr^{-1}). C_1 and C_2 (ppm) denote the gas concentration measured by portable GHG analyzer at t_1 and t_2 (s), respectively. The height of the floating chamber, h, is fixed at 0.4 m. Δt refers to the time interval between t_2 and t_1 (~15 min). V_m is the molar volume of gas, which is taken as 22.4 L·mol^{-1} for this experiment. T_1 is the standard temperature (273 K) and T_2 is the chamber gas temperature. P_1 is the standard atmospheric pressure (101.325 kPa), and P_2 is the chamber gas atmospheric pressure.

Dry weight and carbon content of *M. spicatum*

Monthly collections of *M. spicatum* samples were conducted, with the exception of December 2023, January 2024, and February 2024. The dry weight of *M. spicatum* in each barrel was measured using a sampling survey method with a defined area of 78.5 cm^2. Given that only 1.38% of the sampling area in the barrels was sampled each time, it was deemed that sampling procedure did not significantly perturb the system. The *M. spicatum* samples were manually harvested, with epiphytes removed by rinsing in distilled water. The fresh macrophyte samples were stored at -20°C before being dried in an oven at 50°C until a constant weight was reached. The dry weight was recorded, and the samples were ground and passed through a 100-mesh sieve. The carbon content of *M. spicatum* was then determined using an organic elemental analyzer (Vario UNICUBE, Elementar, German).

Abundance of zooplankton and phytoplankton

Zooplankton and phytoplankton samples were collected once a season (in August and October in 2023 and January and April in 2024). Zooplankton samples were sampled using a 5-L plexiglass water sampler, with a total of 10 L collected in each barrel. These samples were filtered through a plankton net with a mesh size of 64 μm and then preserved in a 4% formaldehyde solution. The two subsamples from each barrel were consolidated into a single sample. The identification of zooplankton genera was conducted using a binocular microscope. The abundance of zooplankton was calculated based on the number and size of individuals [65].

Phytoplankton samples were collected using a plexiglass water sampler to obtain 1 L of surface water, to which 10 mL of Lugol's solution was added for preservation. Following a 48-h settling period in the dark, the samples were siphoned to remove the supernatant. The residual solution was then concentrated to 30 mL and preserved. Identification and enumeration were performed using an optical microscope. The two subsamples from each barrel were pooled into a single sample. The abundance of phytoplankton was calculated by converting the cell density of various genera to volume [19].

Abundance of methanogens and methanotrophs in sediments

Microorganism samples were collected from surface sediments on a quarterly basis in alignment with the zooplankton and phytoplankton sampling schedule, specifically in August and October of 2023, and January and April of 2024. The four replicated samples from each treatment were homogenized to form a single representative sample for that treatment, and then stored in ziplock bags at -20°C. High-throughput sequencing of sediments was conducted to elucidate the specific gene abundance. Quantitative real-time polymerase chain reaction (qPCR) fluorescence quantification was employed to selectively amplify and quantify specific genes (*mcrA* for methanogenic archaea and *pmoA* for methanotrophic bacteria) [24, 25]. The primers employed for the *mcrA* gene were a forward primer MLf (5'- GGTGGTGTMGGATTCACA CARTAYGCWACAGC-3') and a reverse primer MLr (5'-TTCATTGCRTAGTTWGGRTAGTT-3') [30]. For the *pmoA* gene, the primer set included A189f (5'-GGNGAC TGGGACTTCTGG-3') and Mb661r (5'-CCGGMGCA ACGTCYTTACC-3') [7, 18]. For PCR amplification, the cycling conditions were as follows: an initial denaturation step at 95°C for 2 min, 25 cycles (denaturation at 95°C for 30 s, annealing at 55°C for 30 s, and extension at 72°C for 30 s), followed by a final extension at 72°C for 5 min. For the quantitative analysis of methanogens

and methanotrophs, the TB Green fluorescence quantitative PCR kit (Takara, Japan) was applied in conjunction with the aforementioned primers and DNA templates. Quantitative analysis was performed using the QuantiFluor™ST Blue Fluorescence Quantitation System on a NextSeq™ 2000 platform at Personal Biotechnology Co., Ltd (Shanghai, China). Data were analysed using the online platform Genescloud (www.genescloud.cn).

Calculations of carbon stocks in the macrophyte-dominated system

In our study, the primary carbon stocks within the macrophyte-dominated system were categorized into three distinct compartments: macrophyte carbon stock (MCS), water column carbon stock (WCS), and sedimentation carbon stock (SCS). The total carbon stock (TCS) was composed of MCS, WCS, and SCS, with the amount of artificially added carbon (AC) deducted. In a system where macrophytes are dominant, the carbon storage capacity of microorganisms and plankton is significantly lower compared to that of macrophytes. Additionally, the sediments within the system have undergone pre-exposure, and the presence of large benthic animals is minimal. Consequently, the carbon contribution from these organisms was excluded from our study's analysis. The calculation formulas are as follows:

$$\mathrm{MCS} = \mathrm{Weight} \times \mathrm{Carbon\ content}$$

$$\mathrm{WCS} = (\mathrm{TOC} + \mathrm{TIC}) \times V$$

$$\mathrm{SCS} = \frac{SC \times DSW}{A_{beaker} \times t}$$

$$\mathrm{TCS} = \mathrm{MCS} + \mathrm{WCS} + \mathrm{SCS} - \mathrm{AC}$$

where MCS (g C) represents the macrophyte carbon stock at the end of the experiment. Weight (g) is the dry weight of all macrophytes in each barrel at the end of the experiment. WCS (g C) represents the water column carbon stock at the end of the experiment. TOC and TIC (g C L^{-1}) denote their concentrations in water at the end of the experiment, respectively. V (L) is the volume of water in the barrel (450 L). SCS (g C) refers to the sedimentation carbon stock at the end of the experiment. SC (%) represents the total carbon content of sediments, with its determination method detailed in Sect. 2.3. DSW (g) is the dry sediment weight collected in the beaker. A_{beaker} represents the bottom area of the beaker (38.47 cm^{-2}). t (yr) is the duration for which the beaker is placed. TCS (g C) represents the total column carbon stock at the end of the experiment. AC (g C) represents the added carbon.

Statistics

All statistical analyses were performed using R v4.4.2 (R Core Team, 2024). We evaluated the effects of varying HCO_3^- concentrations on each observed variable and GHG diffusive fluxes. Prior to analyzing the response to the addition of HCO_3^-, normality and homogeneity of variance tests were conducted for each variable. The outcomes of these tests dictated the selection of parametric (ANOVA) or non-parametric (Kruskal–Wallis test) methods, followed by the corresponding post-hoc tests. The statistical analyses employed included one-way ANOVA, Welch's ANOVA, and Kruskal–Wallis test, with their respective post-hoc tests being Tukey's HSD test, Games-Howell test, and Dunn test.

To explore the of each observed variable on GHG diffusive fluxes, we utilized the *gamm* and *gam* functions from the "mgcv" package to construct generalized additive mixed models (GAMM) and generalized additive models (GAM), respectively. These models were used to examine the response curves of GHG diffusive fluxes to each observed variable [56]. To minimize the impact of scale differences among predictors and improve the stability and explanatory capacity of the model, the data underwent standardization prior to the construction the GAMM or GAM models. All observed variables were incorporated as fixed effects, with FCH_4 and FCO_2 as the response variables. In GAMM models, different parallel replicates were designated as random effects to account for the intrinsic correlation among them.

The variables exhibiting a significant response to HCO_3^- addition, along with those identified in GAMM or GAM models as having a significant correlation with GHG diffusive flux, were selected for further analysis. These variables were then subjected to Recursive Feature Elimination (RFE) with Random Forests (RF) to determine the key predictors for FCO_2 and FCH_4. RF employed the mean decrease in accuracy (MDA) to calculate the feature importance from the training model of RF-RFE. Functions from the "randomForest" and "rfPermute" packages were employed to construct the RF model and extract variable importance and significance. Variables with the least contribution to model prediction were eliminated, thereby refining the final input feature set through RFE. The variables optimized by RF-RFE were utilized in a Partial Least Squares Path Model (PLS-PM) for causal path analysis, aiming to elucidate the effect of HCO_3^- addition on FCH_4 and FCO_2, as well as to determine the direct and indirect effects of each feature variable on FCH_4 and FCO_2. The *plspm* function from the "plspm" package was employed to construct the PLS-PM model.

Results

Responses of FCH_4 and FCO_2 to HCO_3^- addition

The annual average FCH_4 values were 0.11 ± 0.12 mol m^{-2} yr^{-1} in the control, 0.07 ± 0.05 mol m^{-2} yr^{-1} in the low-level HCO_3^- treatment, 0.07 ± 0.07 mol m^{-2} yr^{-1} in the medium-level HCO_3^- treatment, and 0.07 ± 0.09 mol m^{-2} yr^{-1} in the high-level HCO_3^- treatment, respectively. No significant differences were observed between the different treatments (Fig. 1a). The temporal variation in CH_4 diffusion flux followed a similar pattern across all treatments (Figure S1). In contrast, the FCO_2 showed a significant response to the different levels of HCO_3^- addition (Fig. 1b). The annual average FCO_2 values were -3.48 ± 7.60 mol m^{-2} yr^{-1} in the control, -6.78 ± 5.87 mol m^{-2} yr^{-1} under low HCO_3^- addition conditions, -7.15 ± 8.68 mol m^{-2} yr^{-1} under medium HCO_3^- addition conditions, and -14.04 ± 14.39 mol m^{-2} yr^{-1} under high HCO_3^- addition conditions, respectively (Figure S2).

Responses of other biotic and abiotic variables to HCO_3^- addition

In the treatment with high-level HCO_3^- addition, TP, DTP, Chl-*a*, TOC, and DOC concentrations were significantly elevated compared to the other three treatments ($P < 0.05$), with no significant differences among the latter three (Table S2). The average values of alkalinity, pH, TIC, and DIC also increased with increasing HCO_3^- levels and exhibited significant differences across the different treatments. The addition of HCO_3^- had an influence on the community composition of zooplankton and phytoplankton (Figure S3 and S4); nonetheless, it did not significantly affect their abundance (Table S2). The addition of HCO_3^- led to an increase in the dry weight of *M. spicatum*, with higher levels of HCO_3^- corresponding to significantly great dry weight accumulation ($P < 0.05$). In the treatment with high-level HCO_3^- addition, the annual average dry weight was approximately 2.5 times higher than that in the control. However, carbon content in *M. spicatum* did not show significant responses to HCO_3^- addition.

In the sediments, the absolute abundances of *mcrA* (methanogenic archaea) and *pmoA* (methanotrophic bacteria) genes generally decreased with increasing HCO_3^- addition (Table S2). The absolute abundance of *mcrA* was highest in the control and lowest in the high-level HCO_3^- treatment. A general decline of the abundance of *pmoA* was observed alongside increasing HCO_3^- addition. Despite these downward trends, there were no significant differences in absolute abundance across different treatments.

Correlations between various variables and FCH_4 and FCO_2

The GAMM and GAM models revealed significant correlations between FCH_4 and a range of variables, including water temperature, TP, TOC, DOC, dry weight of *M. spicatum*, abundance of zooplankton and phytoplankton,

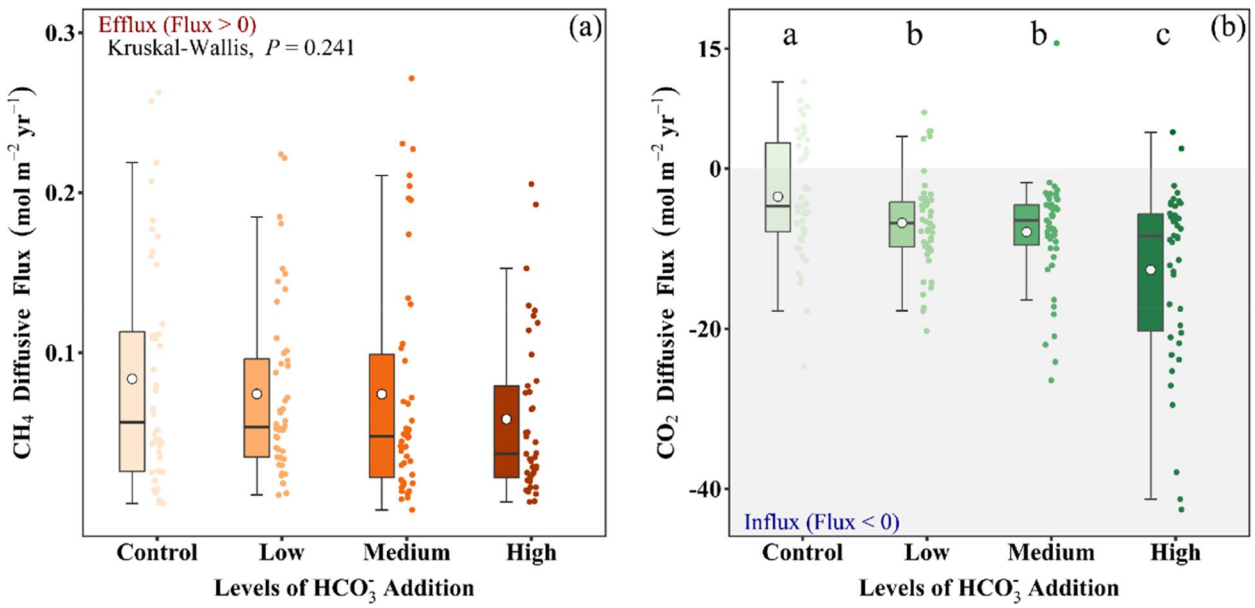

Fig. 1 Annual responses of CH_4 flux (**a**) and CO_2 flux (**b**) to HCO_3^- addition. Values represent mean ± SD ($n = 4$). The whiskers represent the 95% confidence intervals. The categories Control, Low, Medium, and High correspond to HCO_3^- addition levels of 0, 0.5, 1, 2.5 mmol·$L.^{-1}$, respectively. Significant differences between treatments are indicated different letters, with $P < 0.05$

and absolute abundance of *mcrA* (Fig. 2). Notably, the correlation between DOC and FCH_4 was nearly linear (as indicated by a small degree of freedom, $df=1$), whereas the relationships with the other parameters were more complex and nonlinear (Fig. 2 and Table S3). Regarding FCO_2, significant correlations were observed with water temperature, pH, DO, conductance, TN, TP, DTN, alkalinity, dry weight and carbon content of *M. spicatum*, and number of phytoplankton (Fig. 3). Among these, water temperature, pH, DO, conductance, DTN, alkalinity, and dry weight of *M. spicatum* exhibited an overall negative influence on FCO_2, indicating that the reductions in FCO_2 were associated with these parameters.

Key predictors of FCH_4 and FCO_2

According to the RF-RFE analysis, key predictors for FCH_4 were identified as DOC, conductance, TIC, abundance of phytoplankton, DIC, salinity, abundance of *mcrA*, and water temperature, with DOC emerging as the sole statistically significant predictor (Fig. 4). For FCO_2,

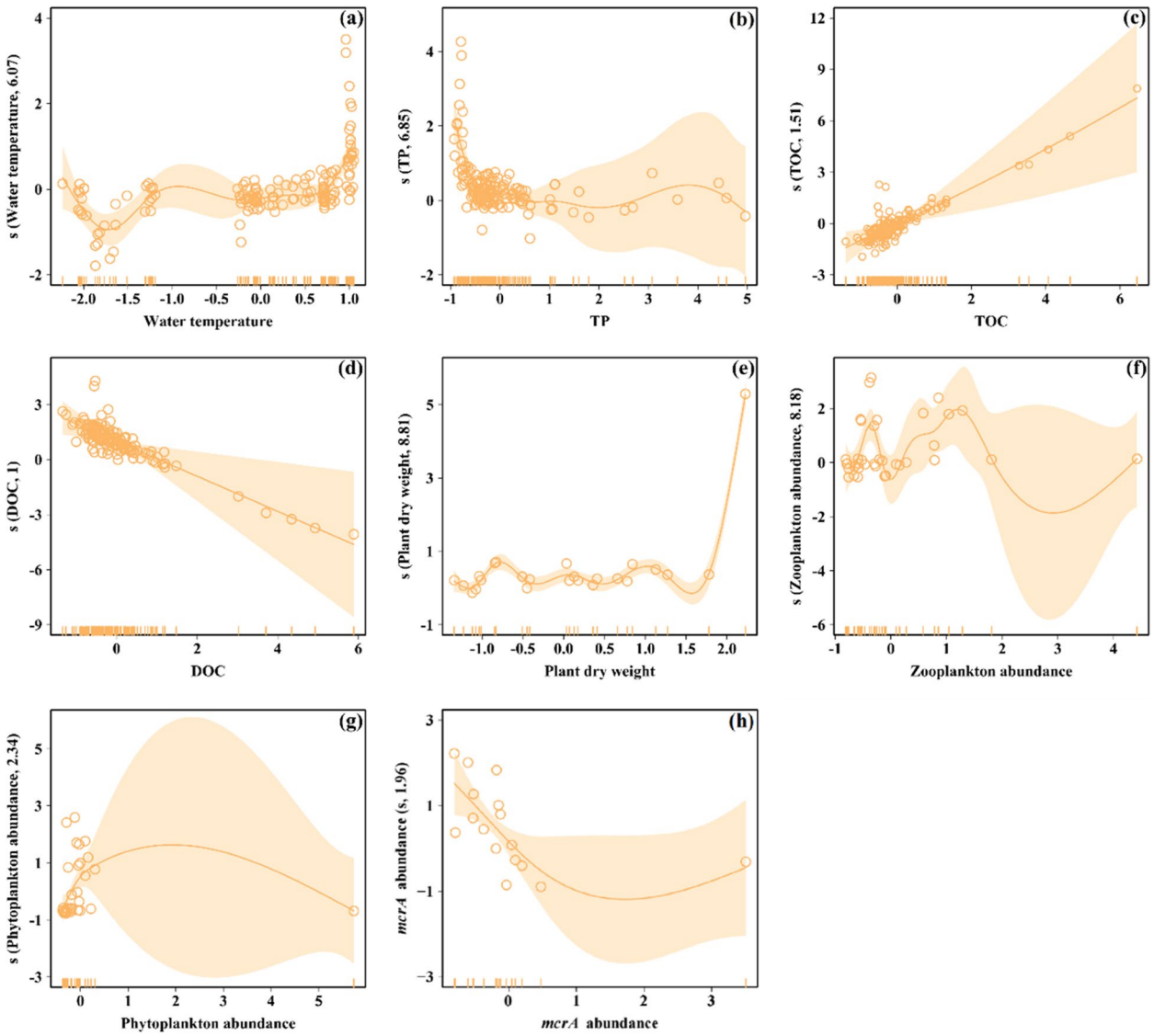

Fig. 2 Generalized Additive Mixed Models (GAMM) and Generalized Additive Models (GAM) results for CH_4 flux. Scatter points represent the residuals between the observed values and the model predictions. The shaded regions encompass the 95% confidence interval. The "rug" along the x-axis and y-axis displays the density of observations. The number adjacent to each y-axis label indicates the effective degrees of freedom for the plotted term. The *y*-axis values indicate *x*-axis covariate effects on deviations from the mean prediction (continuous line). This line represents an estimate of the smooth function of partial residuals, indicating the *x*-axis covariate effects on the measured trait. When the effective degree of freedom equal one, the continuous line is a straight line, indicating a linear effect of the *x*-variable

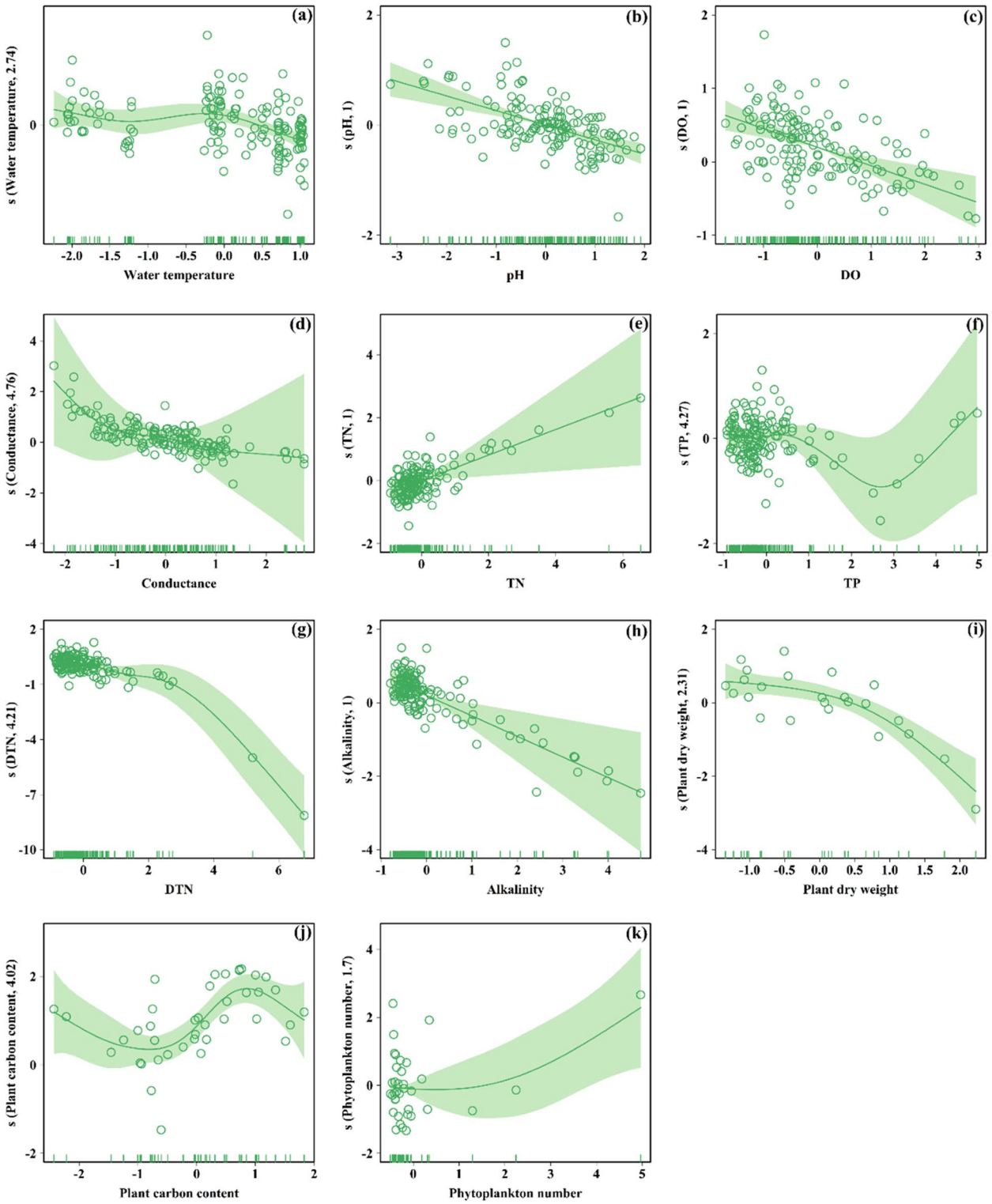

Fig. 3 GAMM and GAM results for CO_2 flux. Scatter points represent the residuals between the observed values and the model predictions

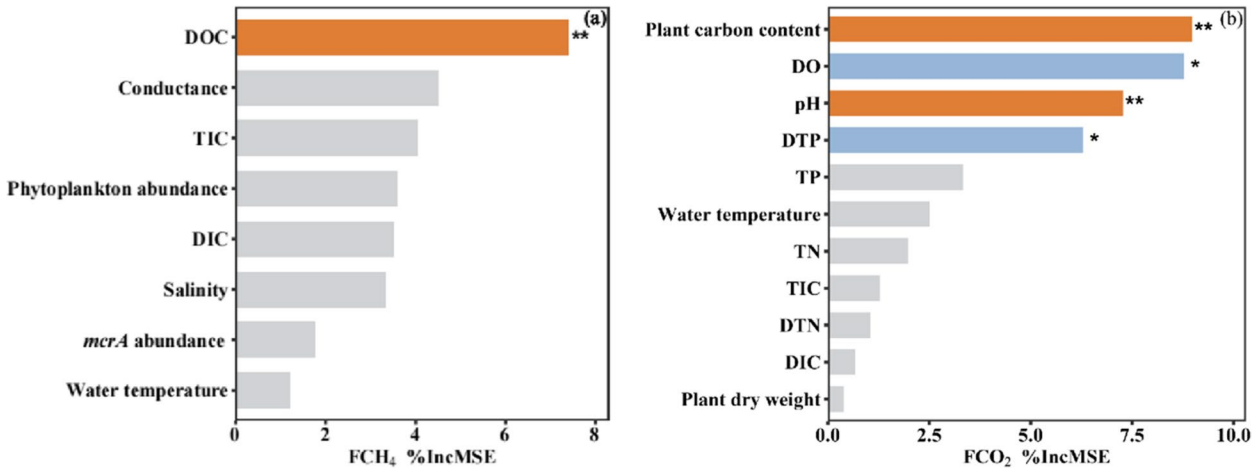

Fig. 4 Random Forest Recursive Feature Elimination (RF-RFE) analysis of the importance of parameters for CH_4 flux (FCH_4) (**a**) and CO_2 flux (FCO_2) (**b**). The x-axis represents the relative feature importance of variables, as calculated by the mean decrease in accuracy (MDA) method, with $^*P < 0.05$ and $^{**}P < 0.01$ in RF analysis

eleven key predictors were identified and the significant predictors were carbon content of *M. spicatum*, DO, pH, and DTP (Fig. 4). The significant predictors from the RF-RFE analysis were incorporated into the PLS-PM analysis as direct influencing variables for FCH_4 and FCO_2, whereas the non-significant were used as indirect influencing variables. The PLS-PM analysis results suggest that the addition of HCO_3^- exerts its regulatory effect on FCH_4 primarily through its influence on DOC, making DOC the predominant direct factor (Fig. 5a and c).

In the PLS-PM model elucidating FCO_2, pH was identified as the predominant direct factor, contributing to 87.69% of the direct influence on FCO_2, with a minor indirect influence of 12.31% (Fig. 5b). Similarly, phosphorus and DO had both direct and indirect effects on FCO_2, with the direct influence being more pronounced (Fig. 5d). In contrast, the carbon content of *M. spicatum* exerted a direct influence on FCO_2 without any discernible indirect impact (Fig. 5d). Post the introduction of HCO_3^-, the combined effect of these factors led to a significant reduction in FCO_2.

Responses of carbon stock to HCO_3^- addition

The addition of HCO_3^- resulted in a significant increase in the water column carbon stock (WCS) and a minor impact on macrophyte carbon stock (MCS) and total carbon stock (TCS), with no effect on sedimentation carbon stock (SCS) (Table S4). With the increase in HCO_3^- addition levels, the proportions of WCS and MCS in TCS increased, while the proportion of SCS gradually decreased (Fig. 6). The response of WCS to HCO_3^- addition was consistent with the changes in TIC and DIC (Table S2). At the end of the experiment, the WCS values for each treatment were 6.67 ± 0.71 g C, 10.41 ± 2.94 g C, 13.75 ± 0.23 g C, and 31.18 ± 5.84 g C, respectively, with significant differences noted between the high-level HCO_3^- addition and the control ($P < 0.05$) (Table S4). Despite an increase in the mean value and proportion of MCS with higher HCO_3^- addition, no significant differences were observed among the treatments at the end of the experiment. Additionally, the addition of HCO_3^- had a negative impact on the proportion of SCS and even led to a slight decrease in sediment carbon accumulation. And the addition of HCO_3^- enhanced the capacity of the total carbon stock of the entire system (Fig. 6 and Table S4).

Discussion

Effects of elevated DIC input on CO_2 and CH_4 fluxes

Rapid carbon cycling in shallow lakes, ponds, and wetlands, compared to deep lakes, is largely attributed to their vulnerability to human activities such as agriculture and urbanization. These activities result in significant inputs of DIC and nutrients within these aquatic ecosystems [20, 66]. Submerged macrophytes have adapted to conditions of low CO_2 availability in aquatic environments by developing physiological structures capable of utilizing DIC and enzymatic systems that utilize HCO_3^-. They can also catalyze the conversion between HCO_3^- and CO_2 through carbonic anhydrase, thus maintaining high photosynthetic rates [29]. Upon exposure to light, the activity of H-ATPase increases, lowering the pH in the epidermis and consequently reducing the HCO_3^-/CO_2 ratio, which allows for the absorption and utilization of more CO_2 [50]. This, in turn, decreases the CO_2 emissions in macrophyte-dominated systems. While

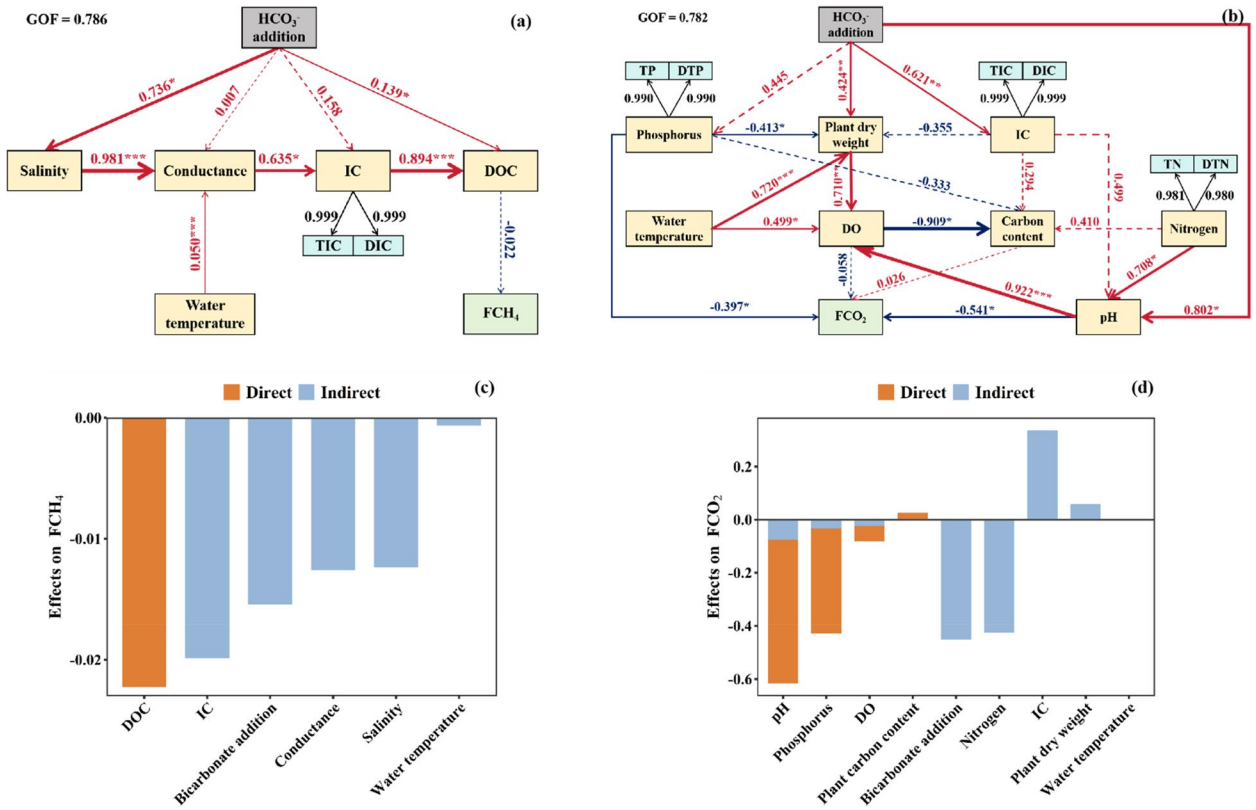

Fig. 5 Partial Least Squares Path Model (PLS-PM) elucidates the impact of HCO_3^- on FCH_4 (**a**) and FCO_2 (**b**). The thickness of the arrows reflects the magnitude of the path coefficients. Solid arrows indicate significant paths, whereas dashed arrows represent non-significant paths. Red and blue lines and numbers correspond to positive and negative paths and their respective strengths. The black numbers signify the loadings of indicators (blue rectangles) onto their corresponding latent variables. "*" ($P < 0.05$) and "**" ($P < 0.01$) indicate that the path coefficients are significant at the 95% confidence level. Standardized direct and indirect effects on FCH_4 (**c**) and FCO_2 (**d**) were derived from the PLS-PM outcomes

acknowledging that an increase in the biomass of macrophytes leads to enhanced accumulation of organic matter, heightened microbial activity, and improved organic matter decomposition efficiency, consequently affecting respiratory activity and CO_2 emissions [53, 64], our findings demonstrate that submerged vegetation substantially diminishes CO_2 fluxes at the water–air interface.

Notably, elevated HCO_3^- concentrations correlate with an increase in macrophyte biomass and a corresponding decrease in CO_2 fluxes (Fig. 1 and Table S2). Short-term studies have indicated that high-density submerged macrophytes exhibit elevated CO_2 concentrations and emissions within microcosms [48]. Other studies have reported that the impact of submerged macrophytes on lake CO_2 emissions is not significant over a three-month period [14, 16]. In contrast, our experimental period spanned one year, encompassing both the growth and decomposition phases of the macrophytes, indicating that systems dominated by submerged macrophytes are beneficial for reducing the system's CO_2 emissions. This finding aligns with previous research conducted in a macrophyte-rich lake [58]. The discrepancies observed in the aforementioned studies could be attributed to the multifaceted impact of submerged plants on CO_2 emissions. Factors such as varying environmental conditions, species and density of submerged plants, and notably, the study duration, are likely to have influenced the outcomes.

Our study revealed that pH, DO, and phosphorus content in the water were negatively correlated with CO_2 fluxes (Fig. 5b), which is consistent with previous findings [45]. As water pH rises from 7.0 to 8.5, the ratio of HCO_3^- to CO_2 concentration increases markedly, from 4 to 140 times [6]. Consequently, submerged macrophytes preferentially utilize HCO_3^- under these conditions. In lakes receiving high DIC inputs, CO_2 emissions are greatly influenced by pH [49]. Our findings confirm that pH is a primary factor affecting CO_2 fluxes with HCO_3^- addition (Fig. 5d). Post HCO_3^- addition, the water pH increased, CO_2 partial pressure decreased, leading to a significant reduction in FCO_2 (Fig. 3). Phosphorus content, particularly DTP,

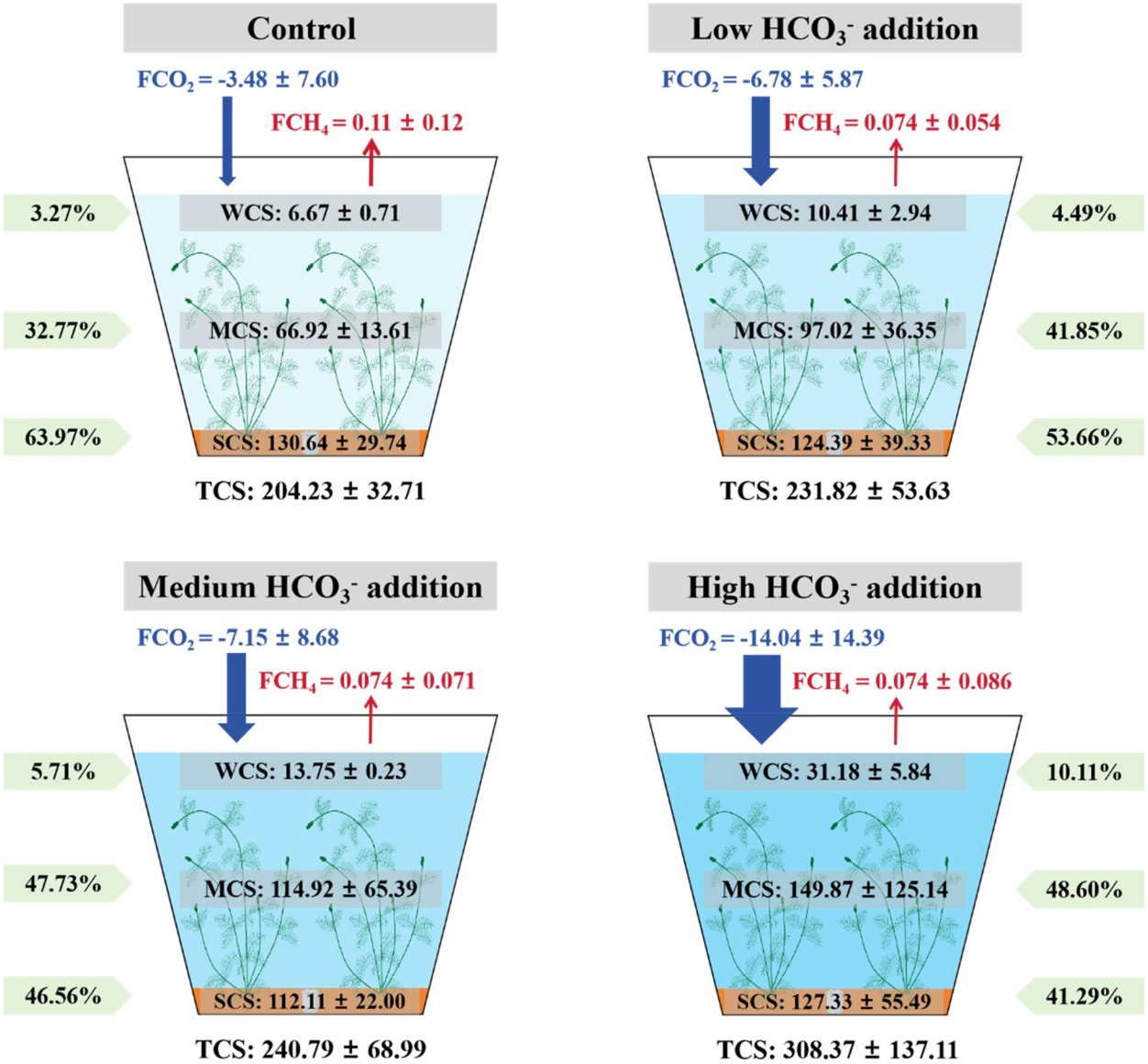

Fig. 6 Summary of carbon stock and CO_2 and CH_4 fluxes (mean ± SD, $n = 4$) under different levels of HCO_3^- addition in macrophyte-dominated systems, with WCS, MCS, SCS and TCS at the end of the experiment in g C, and annual average FCH_4 and FCO_2 in mol m^{-2} yr^{-1}. WCS means water column carbon stock. MCS refers to macrophyte carbon stock. SCS represents sedimentation carbon stock. TCS represents total carbon stock

also significantly impact FCO_2 (Fig. 4b). Phosphorus is an essential nutrient for submerged macrophytes, enhancing CO_2 uptake by boosting primary production [11]. With increased HCO_3^- addition, our study observed a rise in dry weight of macrophyte (Table S2). This could lead to enhanced consumption of dissolved CO_2 and production of DO within aquatic systems, as supported by previous studies [10, 40], thereby reducing CO_2 fluxes and establishing a negative correlation between CO_2 fluxes and the concentrations of DO and phosphorus.

CH_4 in aquatic systems such as lakes and wetlands is primarily produced through the anaerobic decomposition of organic matter by methanogenic archaea in sediments [44]. Additionally, some researchers have indicated that submerged plants can produce methyl compounds that are converted into CH_4 under the influence of reactive oxygen species, and endophytic or epiphytic archaea, algae, cyanobacteria, and proteobacteria on plants can also produce methane in aerobic environments [4, 5, 17, 38, 44]. In our study, as the concentration of HCO_3^- increased, the absolute abundance of the

mcrA gene (methanogenic archaea) in sediments showed a decreasing but non- significant trend. Nonetheless, the abundance of the *pmoA* gene (methanotrophic bacteria) also demonstrated a gradual but non-significant decline (Table S2). Concurrently, CH_4 fluxes also exhibited a downward trend, albeit not significantly (Fig. 1). This finding reflects that submerged plant-dominated systems have a slight mitigating effect on CH_4 emissions; however, this effect is not as pronounced as the reduction in CO_2 emissions.

Oxygen secretion from plant leaves and roots may lead to an increase in DO concentration in both water columns and sediments [40]. In this study, DO concentrations showed a gradual increase with the addition of HCO_3^-, however, this trend was not significant (Table S2), and thus no significant correlation was observed between DO and CH_4 fluxes (Fig. 4). Following the addition of HCO_3^-, DIC can be partially converted into DOC by organisms, and an increase in DOC concentration in water has a direct negative impact on CH_4 emissions (Fig. 5a and c). Submerged macrophytes contain a higher proportion of refractory components, which are prone to forming a refractory carbon pool [54]. One study demonstrated that the annual decomposition rate of submerged plant biomass was less than 50%, suggesting that more than half of the biomass of submerged macrophytes is involved in the carbon sequestration process on an annual basis [26]. Therefore, the increasing DOC concentrations in this study with the gradual addition of HCO_3^- indicate that DOC is not rapidly decomposed and converted into CH_4. Collectively, the results of the one-year experiment showed that the CH_4 emissions from systems dominated by macrophytes were slightly but not significantly inhibited (Fig. 1a). Consequently, even though submerged macrophytes might directly or indirectly produce CH_4, the CH_4 fluxes of the systems did not significantly increase, and even showed a slight decrease. Although some studies have found that CH_4 flux did not significantly change after the harvest of macrophytes [14, 16], our one-year investigation conducted in Lake Xuanwu (Nanjing, China) revealed that in the ecologically restored parts dominated by submerged macrophytes, both CH_4 flux and concentration in the water body were significantly lower than in the unrestored eutrophic parts dominated by phytoplankton [31].

Effects of elevated DIC input on water carbon stock (WCS)

Water carbon stock typically encompasses both inorganic and organic carbon forms. DIC serves as a pivotal reactant and product in the processes of DOC formation and degradation [32, 55]. POC constitutes a minor fraction of the total carbon in aquatic systems, with over 90% of the organic carbon existing in the form of DOC, particularly in marine environments [47]. Particulate organic carbon (POC) is also decomposed by microorganisms into DOC, a significant portion of which is subsequently transformed into refractory components [15]. In our study, the addition of HCO_3^- led to an increase in the organic carbon stock through enhancing the conversion of DIC, thereby expanding the overall capacity of the WCS. Additionally, the elevation of pH due to HCO_3^- addition facilitated the complexation of DOC more with metal ions such as calcium and magnesium, reducing the photodegradation and mineralization rates of DOC [33], and consequently, the capacity of the organic carbon stock was expanded.

After the initial single addition of HCO_3^-, WCS exhibited an increase in the subsequent month (Figure S5). However, this temporary increase was hard to sustain and tended to decline over time. In contrast, with monthly additions of HCO_3^-, WCS not only maintained a high capacity but also showed a tendency of further expansion over time (Figure S5). Macrophytes continuously consumed HCO_3^- during primary production, accelerating the transformation of DIC into DOC [9]. In natural lakes, where watershed DIC typically enters in a continuous manner, the WCS was expected to increase in systems dominated by submerged macrophytes.

Effects of elevated DIC input on macrophyte carbon stock (MCS)

The increase in DIC can accelerate the relative growth rate of some submerged macrophytes and promote more branching [9], enhance biomass [28], and alleviate carbon competition with periphyton [23]. Consequently, in our experiment, the positive response of the MCS on HCO_3^- was observed (Table S2). The increase in DIC concentration led to an increase in MCS capacity, allowing more organic carbon to be stored within MCS and strengthening the carbon sequestration capacity of the entire system (Fig. 6). The carbon fixation capacity of aquatic macrophytes is estimated to be approximately 2.04×10^{18} g yr^{-1}, with a carbon storage amount reaching 1.17×10^{17} g yr^{-1} [35]. In Lake Baoan (Wuhan, China), the dominant macrophyte species *Potamogeton crispus* L. annually sequesters approximately 288 g m^{-2} of carbon [36]. Research indicates that the annual decomposition rate of submerged plant biomass is less than 50%, suggesting that over half of the submerged plant biomass contributes to interannual carbon storage [26]. Consequently, submerged macrophytes represent a substantial carbon reservoir within aquatic ecosystems [36]. In conclusion, in aquatic ecosystems characterized by submerged macrophytes, these plants, via physical, chemical, and biological processes, prolong the carbon turnover time, thereby enhancing carbon sequestration.

Effects of elevated DIC input on sedimentation carbon stock (SCS)

Research indicates that when the total primary productivity carbon content in lakes exceeds 25 g C m^{-2} yr^{-1}, the water body transitions from a carbon sink to a source, releasing the sequestered CO_2 back into the atmosphere. Consequently, in eutrophic lakes, little carbon is effectively buried [21]. As previously discussed, the addition of HCO_3^- directly expanded the WCS and further increases the MCS through photosynthesis. DOC from the WCS, once converted to POC, and a portion of the debris or remains from the MCS and other organisms are eventually deposited and accumulated, thereby inputting into the SCS [8]. In our mesocosm experiment, the annual sedimentation rate (112–131 g C m^{-2}·yr^{-1}) (Fig. 6) fell within the range of sedimentation rates measured in global lake studies (4–400 g C m^{-2}·yr^{-1}, [46, 52]. Sedimentation rates and amounts can be influenced by factors such as temperature, carbon composition, and water trophic status [3, 13].

Notably, our study did not observe significant changes in the sedimentation rate due to HCO_3^- addition at the end of the experiment (Fig. 6). This observation aligns with a previous study attributing such phenomenon to carbon loss resulting from the gradient diffusion of DOC along the continuum of the sediment-pore water-overlying water [27]. More importantly, HCO_3^- addition may have promoted the metabolism of sedimentary carbon, as DIC was positively correlated with sediment respiration rate, implying that microbial carbon metabolic activity in sediments is a significant inorganic carbon source in the water column [60]. In this study, the concentrations of both organic and inorganic carbon in the water column increased with the addition of DIC, also suggesting that carbon decomposition in sediments becomes an important source of both organic and inorganic carbon in the water column (Table S2). Dense macrophyte communities can reduce sediment resuspension [22], which is not only beneficial for maintaining the ecological restoration effects of eutrophic shallow lakes but also for stabilizing the system's sedimentary carbon pool.

Conclusions and implications

Our findings demonstrated that increased HCO_3^- addition reduced CO_2 fluxes in *M. spicatum*-dominated systems. Both direct and indirect effects on FCO_2 were observed due to variations in pH, phosphorus, and DO. The carbon content of *M. spicatum* exerted a direct influence on CO_2 fluxes without any discernible indirect impact. Unlike changes in CO_2 fluxes, the addition of HCO_3^- had no significant effect on CH_4 fluxes. There were no significant differences in absolute abundance of *mcrA* and *pmoA* genes across different HCO_3^- addition treatments. The regulatory effect of HCO_3^- addition on CH_4 fluxes was primarily through its influence on DOC. Enhanced DIC inputs expanded the capacity for water carbon stocks and macrophyte carbon stocks. While CH_4 fluxes and carbon sedimentation stocks were not significantly impacted, the overall carbon sink function of macrophyte-dominated systems was enhanced.

As climate warming intensifies, the reduction of greenhouse gas emissions becomes increasingly urgent, and the utilization of natural ecosystems for carbon storage has emerged as a focal point of global concern. Our findings in this study underscore the importance of submerged macrophyte-dominated aquatic ecosystems in mitigating CO_2 and CH_4 emissions and enhancing system carbon stocks. Our data reveal that both CO_2 and CH_4 fluxes in the macrophyte-dominated regions of Lake Xuanwu are significantly lower than in phytoplankton-dominated areas, as previously reported [31]. The ongoing restoration efforts focused on submerged plants in shallow lakes are crucial in this context, especially given the continuous influx of DIC and nutrients from the watershed into the lakes. These initiatives not only facilitate the restoration of clear water states in lakes but also augment the lakes' carbon storage capacity. Therefore, adopting effective measures to preserve and enhance the carbon sequestration potential of ecosystems, such as lakes and wetlands, is imperative for bolstering the global carbon sink and alleviating the impacts of climate warming.

Supplementary Information

The online version contains supplementary material available at https://doi.org/10.1186/s12870-025-06651-2.

Supplementary Material 1.

Acknowledgements

We thank Xiaolong Huang, Zhaoshi Wu, Hu He and You Zhang for fruitful discussions, Guijun Yang for his technical assistance during the experiment. We would like to express our gratitude to Fenlan Chen and Lanying Chen for field and laboratory assistance. We also extend our gratitude to Liangpeng Qi and Jun Yu from Shiyanjia Lab (www.shiyanjia.com) for providing assistance with TOC analysis.

Author's contributions

KYL, YLS, BHG, and FD made substantial contributions to the conception and design of the work. FD, AA, WJQ, and TQ completed the experiment and made the acquisition, analysis, and interpretation of data. FD drafted the work and YLS substantively revised it.

Funding

The National Science Foundation of China (32330068, 32471640, and 32171534) and Jiangsu Provincial Science and Technology Planning Project (BK20231515 and BK20231516) supported this publication.

Data availability

The datasets generated during this study are available from the corresponding author upon reasonable request.

Declarations

Ethics approval and consent to participate
Not applicable.

Consent for publication
We confirm that all authors have reviewed and approved the final version of this manuscript and consent to its publication.

Competing interests
The authors declare no competing interests.

Received: 17 March 2025 Accepted: 29 April 2025
Published online: 10 May 2025

References

1. Angle JC, Morin TH, Solden LM, Narrowe AB, Smith GJ, Borton MA, et al. Methanogenesis in oxygenated soils is a substantial fraction of wetland methane emissions. Nat Commun. 2017;8:1567.
2. Baliña S, Sánchez ML, Izaguirre I, del Giorgio PA. Shallow lakes under alternative states differ in the dominant greenhouse gas emission pathways. Limnol Oceanogr. 2023;68:1–13.
3. Berthold M, Paar M. Dynamics of primary productivity in relation to submerged vegetation of a shallow, eutrophic lagoon: a field and mesocosm study. PLoS ONE. 2021;16:e0247696.
4. Bižić-Ionescu M, Ionescu D, Günthel M, Tang KW, Grossart HP. Oxic methane cycling: new evidence for methane formation in oxic lake water. Biogen Hydrocarbons. 2018;2018:1–22.
5. Bogard MJ, Del Giorgio PA, Boutet L, Chaves MCG, Prairie YT, Merante A, Derry AM. Oxic water column methanogenesis as a major component of aquatic CH_4 fluxes. Nat Commun. 2014;5:5350.
6. Boyd CE, Boyd CE. Carbon dioxide, pH, and alkalinity. Water Qual. 2020;52:177–203.
7. Costello AM, Lidstrom ME. Molecular characterization of functional and phylogenetic genes from natural populations of methanotrophs in lake sediments. Appl Environ Microbiol. 1999;65:5066–74.
8. Fan LF, Kang EC, Natividad MB, Hung CC, Shih YY, Huang WJ, Chou WC. The role of benthic TA and DIC fluxes on carbon sequestration in seagrass meadows of Dongsha Island. J Marine Sci Eng. 2024;12:2061.
9. Fasoli JVB, Mormul RP, Cunha ER, Thomaz SM. Plasticity responses of an invasive macrophyte species to inorganic carbon availability and to the interaction with a native species. Hydrobiologia. 2018;817:227–37.
10. Feijoó C, Arroita M, Messetta ML, Anselmo J, Rigacci L, Von Schiller D. Patterns and controls of carbon dioxide concentration and fluxes at the air–water interface in South American lowland streams. Aquat Sci. 2022;84:23.
11. Feng W, Wang T, Zhu Y, Sun F, Giesy JP, Wu F. Chemical composition, sources, and ecological effect of organic phosphorus in water ecosystems: a review. Carbon Res. 2023;2:12.
12. Gao Y, Jia J, Lu Y, Yang T, Lyu S, Shi K, et al. Determining dominating control mechanisms of inland water carbon cycling processes and associated gross primary productivity on regional and global scales. Earth Sci Rev. 2021;213:103497.
13. Gonzalez Rodriguez L, McCallum A, Kent D, Rathnayaka C, Fairweather H. A review of sedimentation rates in freshwater reservoirs: recent changes and causative factors. Aquat Sci. 2023;85:60.
14. Gremmen T, van Dijk G, Postma J, Colina M, de SenerpontDomis LN, Velthuis M, et al. Factors influencing submerged macrophyte presence in fresh and brackish eutrophic waters and their impact on carbon emissions. Aquatic Botany. 2023;187:103645.
15. Hansell DA, Carlson CA. Localized refractory dissolved organic carbon sinks in the deep ocean. Global Biogeochem Cycles. 2013;27:705–10.
16. Harpenslager SF, Thiemer K, Levertz C, Misteli B, Sebola KM, Schneider SC, et al. Short-term effects of macrophyte removal on emission of CO_2 and CH_4 in shallow lakes. Aquatic Botany. 2022;182:103555.
17. Hilt S, Grossart HP, McGinnis DF, Keppler F. Potential role of submerged macrophytes for oxic methane production in aquatic ecosystems. Limnol Oceanogr. 2022;67:S76–88.
18. Holmes AJ, Costello A, Lidstrom ME, Murrell JC. Evidence that participate methane monooxygenase and ammonia monooxygenase may be evolutionarily related. FEMS Microbiol Lett. 1995;132:203–8.
19. Hu, H. (Ed.). (2006). The freshwater algae of China: systematics, taxonomy and ecology. Science press.
20. Huang Y, Song X, Wang YP, Canadell JG, Luo Y, Ciais P, et al. Size, distribution, and vulnerability of the global soil inorganic carbon. Science. 2024;384:233–9.
21. Huntley ME, Lopez MDG, Karl DM. Response: carbon and the antarctic marine food web. Science. 1992;257:259–60.
22. Jeppesen, E., Søndergaard, M., Søndergaard, M., & Christoffersen, K. (Eds.). (2012). The structuring role of submerged macrophytes in lakes (Vol. 131). Springer Science & Business Media.
23. Jones JI, Young JO, Eaton JW, Moss B. The influence of nutrient loading, dissolved inorganic carbon and higher trophic levels on the interaction between submerged plants and periphyton. J Ecol. 2002;90:12–24.
24. Juottonen H, Galand PE, Yrjälä K. Detection of methanogenic Archaea in peat: comparison of PCR primers targeting the mcrA gene. Res Microbiol. 2006;157:914–21.
25. Knief C. Diversity and habitat preferences of cultivated and uncultivated aerobic methanotrophic bacteria evaluated based on pmoA as molecular marker. Front Microbiol. 2015;6:1346.
26. Li W, Chen K, Wu Q, Pan J. Experimental studies on decomposition process of aquatic plant material from East Taihu Lake. J Lake Sci. 2001;13:331–6.
27. Li Y, Chao C, Zuo Z, Hu J, Yu H, Liu C, Yu D. Effects of dissolved inorganic level and sediment types on the plant traits of Myriophyllum spicatum L. and its exudates input to sediment. Aquatic Sci. 2023;85:24.
28. Li Y, He Q, Ma X, Wang H, Liu C, Yu D. Plant traits interacting with sediment properties regulate sediment microbial composition under different aquatic DIC levels caused by rising atmospheric CO_2. Plant Soil. 2019;445:497–512.
29. Lin Q, Wang SL. The composition of stable carbon isotope and some influencing factors of submerged plant. Acta Ecol Sin. 2001;21:806–9.
30. Luton PE, Wayne JM, Sharp RJ, Riley PW. The mcrA gene as an alternative to 16S rRNA in the phylogenetic analysis of methanogen populations in landfill. Microbiology. 2002;148:3521–30.
31. Mei, Y. K., Su, Y. L., Dong, Z. G., Fan, S. M., Li, K. Y., Xing, P., Wu, Q. L. (2025). Ecological restoration impacts on water quality and carbon-based greenhouse gas emissions: a case study of Lake Xuanwu. Journal of Lake Sciences, in press.
32. Minor EC, Oyler AR. Dissolved organic matter in large lakes: a key but understudied component of the carbon cycle. Biogeochemistry. 2023;164:295–318.
33. Pace ML, Reche I, Cole JJ, Fernández-Barbero A, Mazuecos IP, Prairie YT. pH change induces shifts in the size and light absorption of dissolved organic matter. Biogeochemistry. 2012;108:109–18.
34. Pagano AM, Titus JE. Submersed macrophyte growth at low pH: carbon source influences response to dissolved inorganic carbon enrichment. Freshw Biol. 2007;52:2412–20.
35. Pal S, Chattopadhyay B, Datta S, Mukhopadhyay SK. Potential of wetland macrophytes to sequester carbon and assessment of seasonal carbon input into the East Kolkata Wetland Ecosystem. Wetlands. 2017;37:497–512.
36. Pan WB, Cai QH. The function of the macrophyte in the carbon circulation of Baoan Lake. Acta Hydrobiol Sin. 2000;24:425–8.
37. Pedersen O, Colmer TD, Sand-Jensen K. Underwater photosynthesis of submerged plants–recent advances and methods. Front Plant Sci. 2013;4:140.
38. Perez-Coronel E, Michael Beman J. Multiple sources of aerobic methane production in aquatic ecosystems include bacterial photosynthesis. Nat Commun. 2022;13:6454.
39. Poschenrieder C, Fernández JA, Rubio L, Pérez L, Terés J, Barceló J. Transport and use of bicarbonate in plants: current knowledge and challenges ahead. Int J Mol Sci. 2018;19:1352.
40. Rabaey JS, Domine LM, Zimmer KD, Cotner JB. Winter oxygen regimes in clear and turbid shallow lakes. J Geophys Res. 2021;126:e2020JG006065.

41. Raven JA, Beardall J. CO_2 concentrating mechanisms and environmental change. Aquat Bot. 2014;118:24–37.
42. Repeta DJ, Ferrón S, Sosa OA, Johnson CG, Repeta LD, Acker M, et al. Marine methane paradox explained by bacterial degradation of dissolved organic matter. Nat Geosci. 2016;9:884–7.
43. Rice EW, Baird RB, Eaton AD, Clesceri LS. Standard methods for the examination of water and wastewater. 2012.
44. Rosentreter JA, Borges AV, Deemer BR, Holgerson MA, Liu S, Song C, et al. Half of global methane emissions come from highly variable aquatic ecosystem sources. Nat Geosci. 2021;14:225–30.
45. Sun H, Lu X, Yu R, Yang J, Liu X, Cao Z, et al. Eutrophication decreased CO_2 but increased CH_4 emissions from lake: a case study of a shallow Lake Ulansuhai. Water Res. 2021;201:117363.
46. Tartari G, Biasci G. Trophic status and lake sedimentation fluxes. Water Air Soil Pollut. 1997;99:523–31.
47. Temmink RJ, Lamers LP, Angelini C, Bouma TJ, Fritz C, van de Koppel J, et al. Recovering wetland biogeomorphic feedbacks to restore the world's biotic carbon hotspots. Science. 2022;376:eabn1479.
48. Theus ME, Ray NE, Bansal S, Holgerson MA. Submersed macrophyte density regulates aquatic greenhouse gas emissions. J Geophys Res. 2023;128:e2023JG007758.
49. Tranvik LJ, Downing JA, Cotner JB, Loiselle SA, Striegl RG, Ballatore TJ, et al. Lakes and reservoirs as regulators of carbon cycling and climate. Limnol Oceanograp. 2009;54:2298–314.
50. Van TK, Haller WT, Bowes G. Comparison of the photosynthetic characteristics of three submersed aquatic plants. Plant Physiol. 1976;58:761–8.
51. Vasistha P, Ganguly R. Water quality assessment of natural lakes and its importance: an overview. Mater Today. 2020;32:544–52.
52. Velthuis M, Kosten S, Aben R, Kazanjian G, Hilt S, Peeters ET, et al. Warming enhances sedimentation and decomposition of organic carbon in shallow macrophyte-dominated systems with zero net effect on carbon burial. Global Change Biol. 2018;24:5231–42.
53. Wada K, Kishimoto N, Somiya I, Sato T, Ueno K. Impact of submerged macrophytes on behavior of organic carbon and nutrients: an experimental study. J Water Environ Technol. 2021;19:35–47.
54. Wang S, Gao Y, Jia J, Kun S, Lyu S, Li Z, et al. Water level as the key controlling regulator associated with nutrient and gross primary productivity changes in a large floodplain-lake system (Lake Poyang), China. J Hydrol. 2021;599:126414.
55. Wetzel RG. Detritus: organic carbon cycling and ecosystem metabolism. Limnology. 2001:731–783.
56. Wood, S. N. (2017). Generalized additive models: an introduction with R: chapman and hall/CRC.
57. Xie J, Gao Y, Xu X, Chen T, Tian L, Zhang C, et al. Effects of decomposition of submerged aquatic plants on CO_2 and CH_4 release in river sediment–water environment. Water. 2023;15:2863.
58. Xing Y, Xie P, Yang H, Wu A, Ni L. The change of gaseous carbon fluxes following the switch of dominant producers from macrophytes to algae in a shallow subtropical lake of China. Atmos Environ. 2006;40:8034–43.
59. Xu X, Wu C, Xie D, Ma J. Sources, migration, transformation, and environmental effects of organic carbon in eutrophic lakes: a critical review. Int J Environ Res Public Health. 2023;20:860.
60. Xu Y, Wei Q, Wei Z, Ruan A. Key roles of carbon metabolic intensity of sediment microbes in dynamics of algal blooms in shallow freshwater lakes. Hydrobiologia. 2024;851:1–17.
61. Xun F, Li B, Chen H, Zhou Y, Gao P, Xing P. Effect of salinity in alpine lakes on the southern Tibetan Plateau on greenhouse gas diffusive fluxes. J Geophys Res. 2022;127:e2022JG006984.
62. Yin L, Li W, Madsen TV, Maberly SC, Bowes G. Photosynthetic inorganic carbon acquisition in 30 freshwater macrophytes. Aquat Bot. 2017;140:48–54.
63. Yvon-Durocher G, Hulatt CJ, Woodward G, Trimmer M. Long-term warming amplifies shifts in the carbon cycle of experimental ponds. Nat Clim Chang. 2017;7:209–13.
64. Zhang C, Xing B, Zuo Z, Lv T, Chao C, Li Y, et al. Drivers of organic carbon stocks in eutrophic lake sediments after reestablishment of submerged aquatic vegetation. Plant and Soil. 2024;499:639–53.
65. Zhang ZS, Huang XF. Methodology of freshwater plankton research. Beijing: Science Press; 1991.
66. Zhou J, Leavitt PR, Zhang Y, Qin B. Anthropogenic eutrophication of shallow lakes: is it occasional? Water Res. 2022;221:118728.

Publisher's Note